E I S A
European Institute for Sciences and Their Applications

The Dark Side of the Universe - DSU2024
SEPTEMBER 8 - 14, 2024

Gravitational Waves from (Melting) Domain Walls

Alexander Vikman

09.09.2024

Co-funded by the European Union
MINISTRY OF EDUCATION, YOUTH AND SPORTS
FZU Institute of Physics of the Czech Academy of Sciences
ceico
GAČR CZECH SCIENCE FOUNDATION

This talk is based on

- Beyond freeze-in: dark matter via inverse phase transition and gravitational wave signal
  `e-Print: 2104.13722, PRD`

- Gravitational shine of dark domain walls
  `e-Print: 2112.12608, JCAP`

- NANOGrav spectral index γ=3 from melting domain walls
  `e-Print: 2307.04582, PRD`

- Revisiting evolution of domain walls and their gravitational radiation with CosmoLattice
  `e-Print: 2406.17053, JCAP accepted today`

Eugeny Babichev (IJCLab, Orsay)
Ivan Dankovsky (Moscow State U. and INR)
Dmitry Gorbunov (INR and MIPT, Moscow)
Sabir Ramazanov (ITMP, Moscow State U.)
Rome Samanta (INFN & SSM, Naples)
Alexander Vikman (CEICO, FZU Prague)

Main Message

- Ultralight DM can be created for minuscular couplings and still produce observable GW

- NANOGrav GW can be from Melting Domain Walls of

- Scaling Regime in DW evolution seems to be only a local attractor,

Z_2 -symmetric DM scalar field χ coupled to ϕ - a multiplet of N *thermal* degrees of freedom

portal coupling

$$V = \frac{1}{2}\left(M^2 - g^2\phi^\dagger\phi\right)\cdot\chi^2 + \frac{\lambda}{4}\chi^4 + \frac{\lambda_\phi}{4}\left(\phi^\dagger\phi\right)^2$$

tachyonic thermal mass

$$\mu^2 = g^2\langle\phi^\dagger\phi\rangle \simeq \frac{Ng^2T^2}{12}$$

increasing during preheating, then red-shifting

potential bounded from below

$$\beta = \frac{\lambda}{g^4} \geq \frac{1}{\lambda_\phi} \geq 1$$

potential bounded from below

weak coupling

Direct Phase Transition

Early universe spontaneously Broken Phase

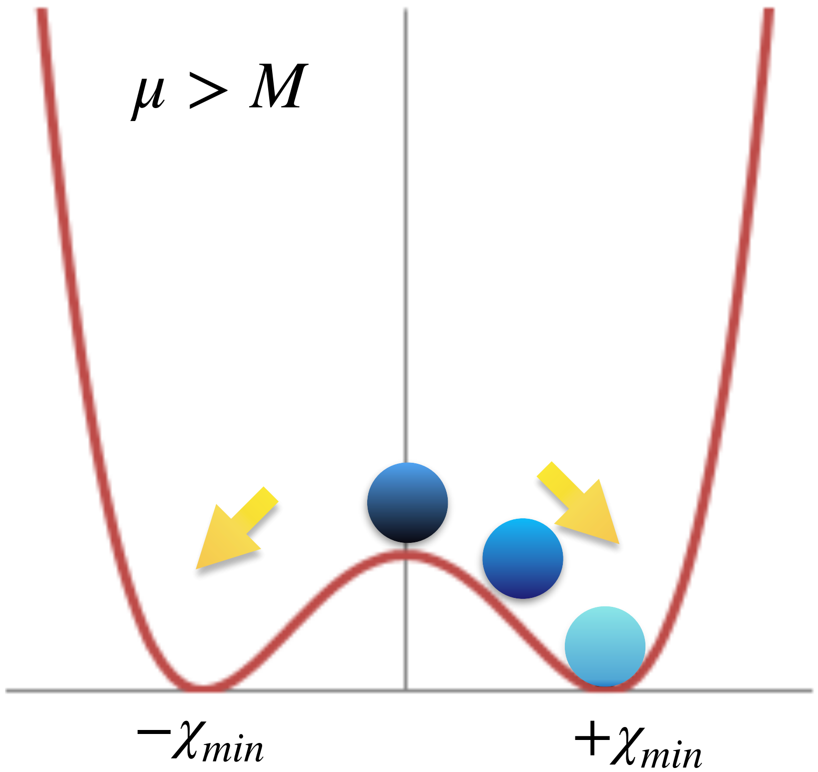

Avoid too much friction to start rolling

$$\mu \gtrsim H$$

$$\sqrt{\frac{N}{12}} g T_i \simeq \sqrt{\frac{\pi^2 g_*}{90}} \frac{T_i^2}{M_{pl}}$$

$$T_i \simeq g\, M_{Pl} \sqrt{\frac{N}{g_*(T_i)}} \times \frac{1}{\sqrt{B}}$$

Correction taking into account time to get to the minimum

Domain Walls!

$$V_{eff} \simeq \frac{\lambda \cdot \left(\chi^2 - \eta^2\right)^2}{4} \qquad \eta(T) \simeq g\sqrt{\frac{N}{12\lambda}}\, T$$

Tension/energy per unit surface $\sigma_{wall} = \frac{2\sqrt{2\lambda}}{3}\eta^3(T)$ melting away as $\propto T^3$!

In the **scaling regime (Kibble 1976):** one domain wall per Hubble volume:

$$M_{wall} \sim \sigma_{wall}/H^2$$

$$\rho_{wall} \sim M_{wall} H^3 \sim \sigma_{wall}\, H \propto T^5$$

Usual Constant tension DW
$\rho_{wall} \propto T^2$

Let us first study **usual constant tension** DW and associated GW

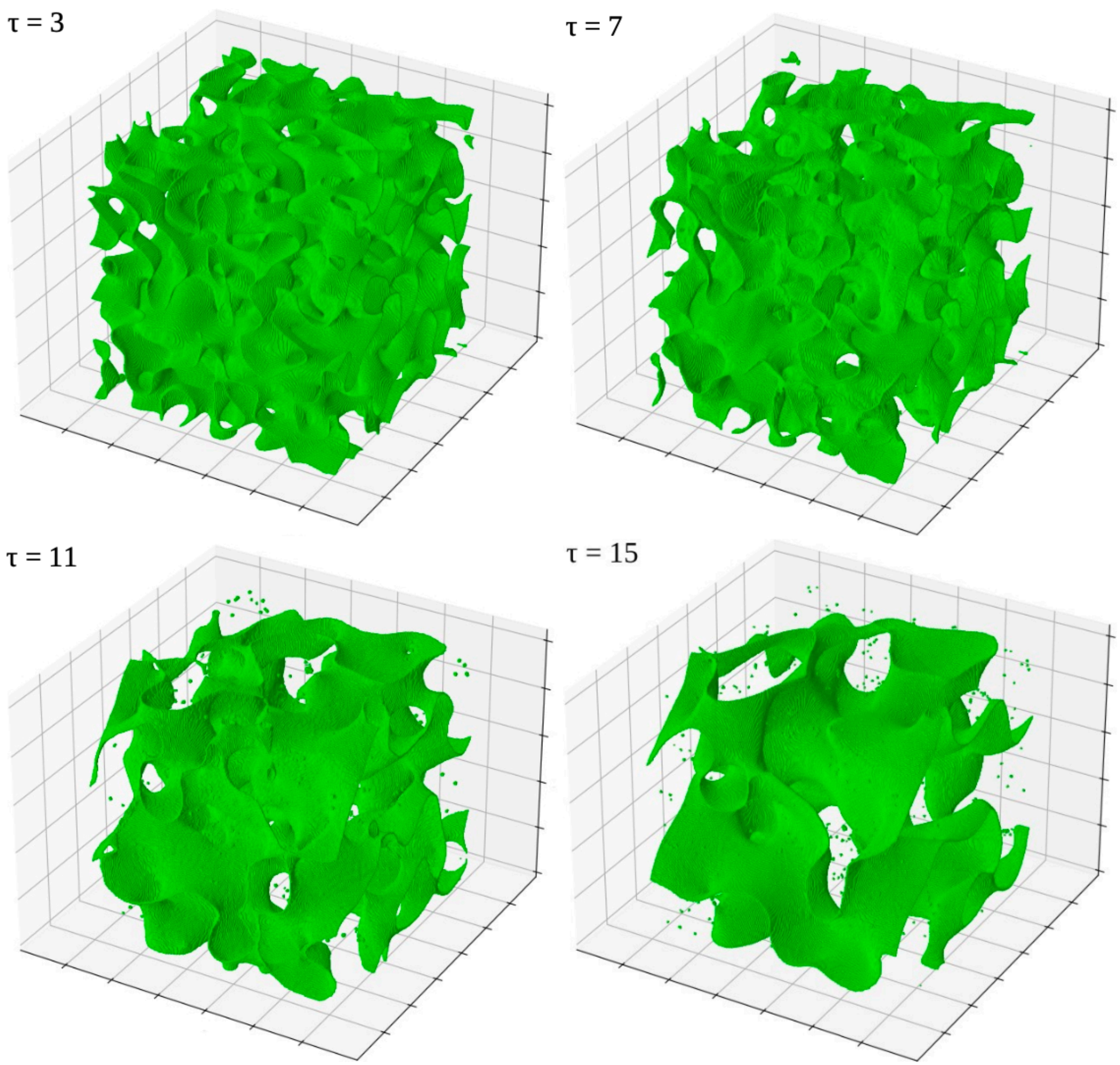

Figure 2: Snapshots of domain wall evolution in the case of vacuum initial conditions at different conformal times τ in units of $\frac{1}{\sqrt{\lambda}\eta}$. Simulations have been performed starting from vacuum initial conditions on a lattice with the grid number $N = 512$. The visible dot-like structures are small size domain walls.

Dankovsky, Babichev, Gorbunov, Ramazanov, Vikman (2024)

Figueroa, Florio, Torrenti, Valkenburg

CosmoLattice

"vacuum" initial conditions

$$\left\langle \chi(\mathbf{k})\chi^*(\mathbf{k}')\right\rangle = \frac{1}{2k}\delta(\mathbf{k}-\mathbf{k}')$$

$$\left\langle \dot\chi(\mathbf{k})\dot\chi^*(\mathbf{k}')\right\rangle = \frac{k}{2}\delta(\mathbf{k}-\mathbf{k}')$$

"thermal" initial conditions

$$\times\frac{2}{e^{k/T}-1}$$

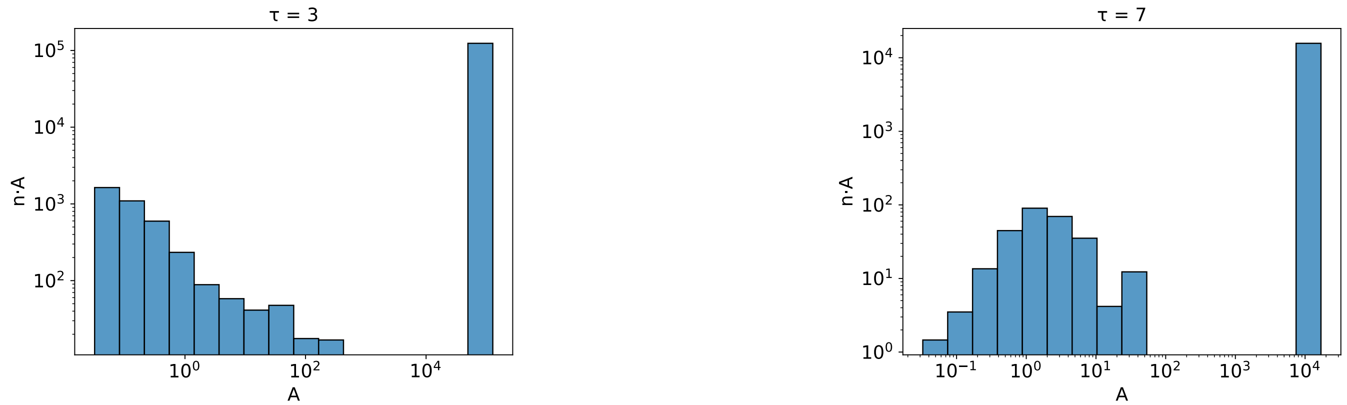

Figueroa, Florio,
Torrenti, Valkenburg

CosmoLattice

Dankovsky,
Babichev,
Gorbunov,
Ramazanov,
Vikman
(2024)

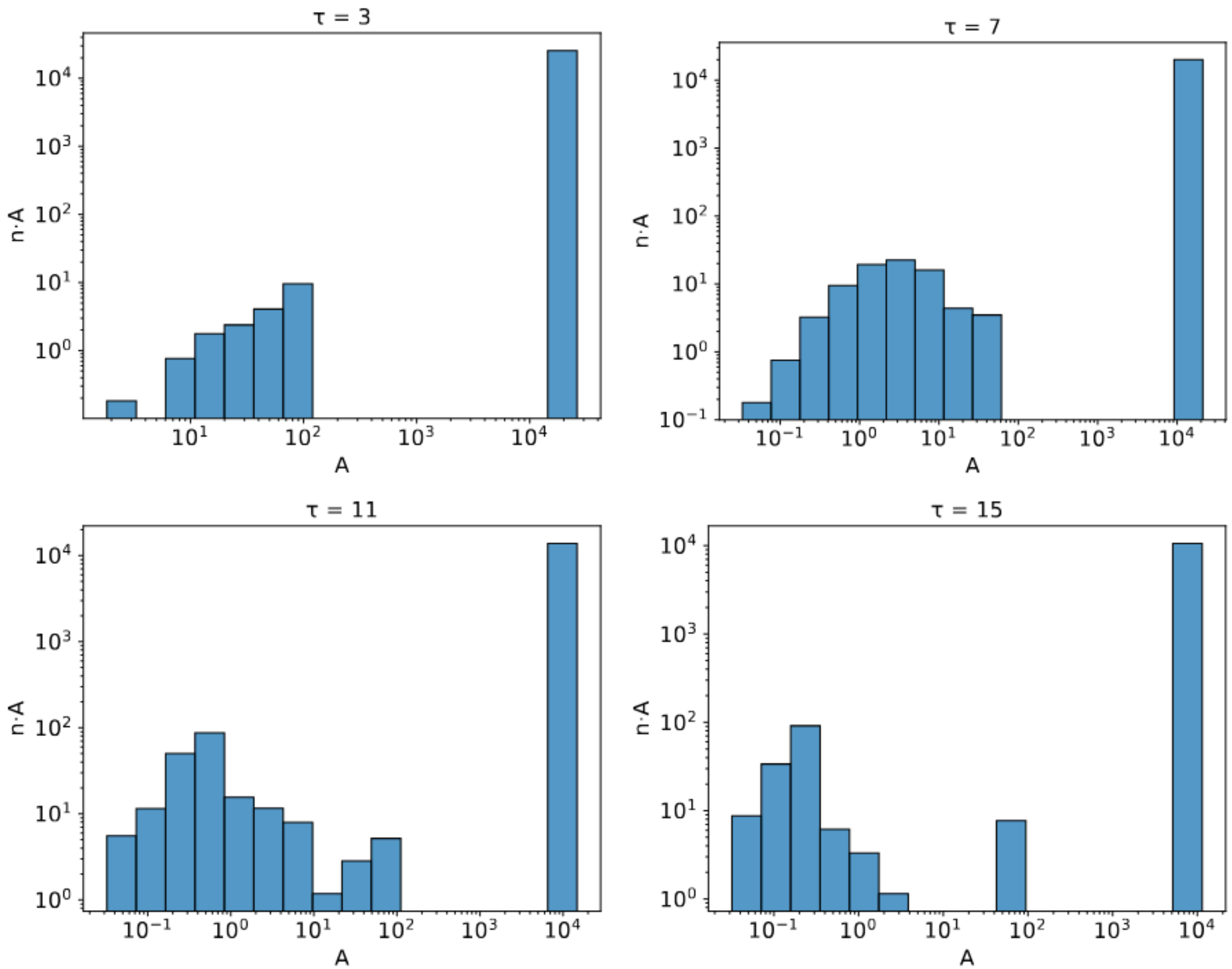

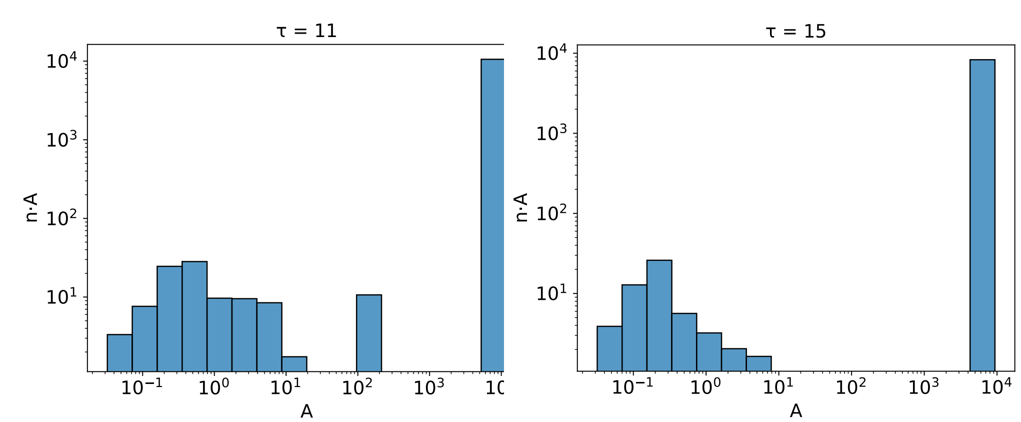

Figure 5: Histograms showing the distribution of the quantity $n \cdot A$ versus A, where A is the comoving domain wall area in units of $\frac{1}{\lambda \eta^2}$, and n is the number of domain walls with the area A. Distributions are considered at different conformal times τ in units of $\frac{1}{\sqrt{\lambda}\eta}$. Simulations have been performed starting from vacuum initial conditions on a lattice with the grid number $N = 512$.

Scaling Parameter (constant tension DW)

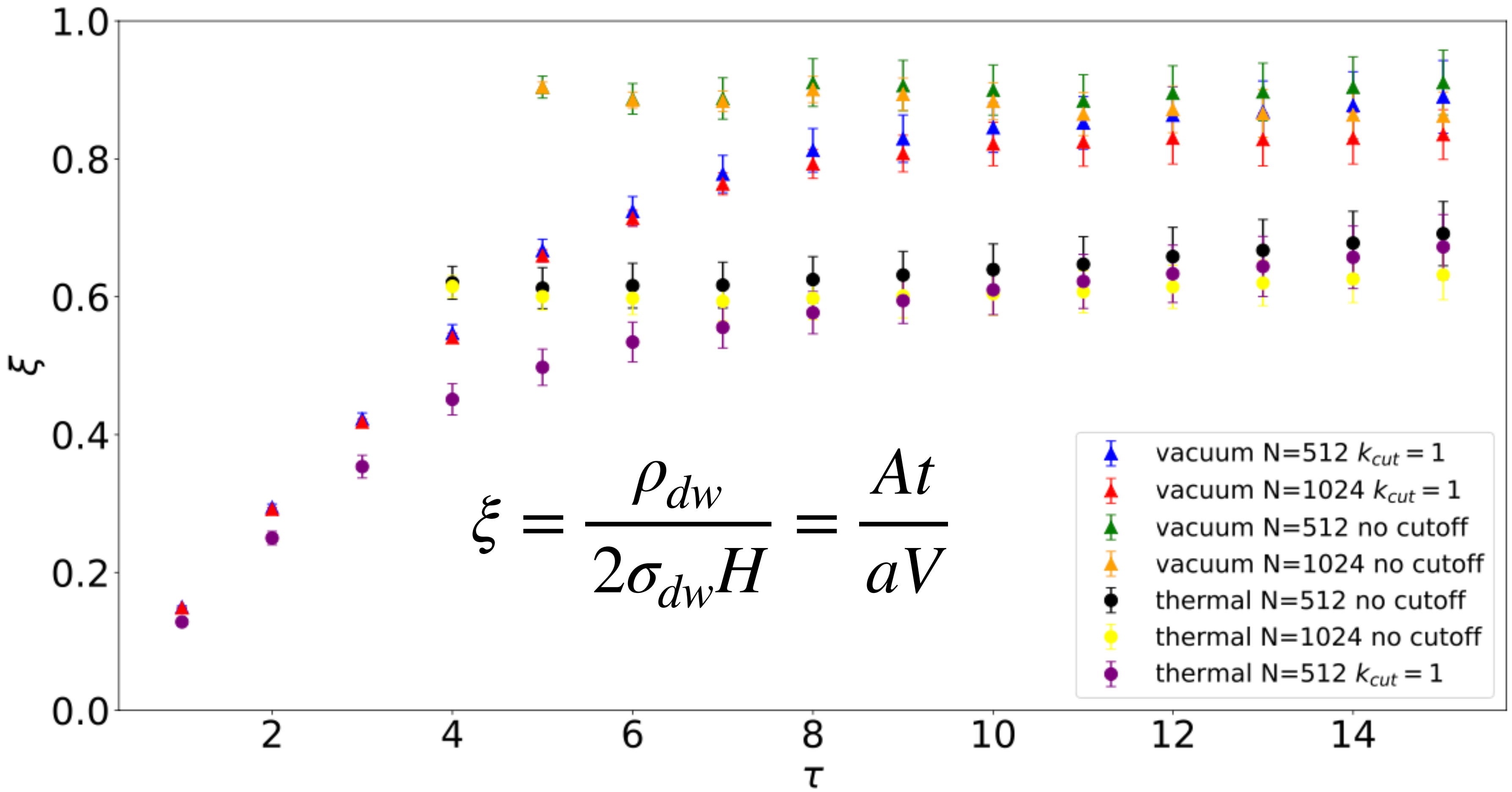

Figure 4: The area parameter ξ inferred in Eq. (44) is obtained from numerical simulations performed on lattices with the grid numbers $N = 512$ and $N = 1024$ starting from vacuum and thermal initial conditions with and without cutoffs at high momenta. Conformal time τ and conformal momentum k are in units of $\frac{1}{\sqrt{\lambda}\eta}$ and $\sqrt{\lambda}\eta$, respectively. The parameter ξ taking a constant value reflects that the domain wall network enters the scaling regime. Expectation values and error bars are obtained from 10 simulations run with different base seed values.

Figueroa, Florio, Torrenti, Valkenburg

CosmoLattice

Dankovsky, Babichev, Gorbunov, Ramazanov, Vikman (2024)

Cf. Hiramatsu, Kawasaki, Saikawa (2013);
Ferreira, Gasparotto, Hiramatsu, Obata, Pujolas (2023);
Kitajima, Lee, Takahashi, Yin (2023)

GW energy density

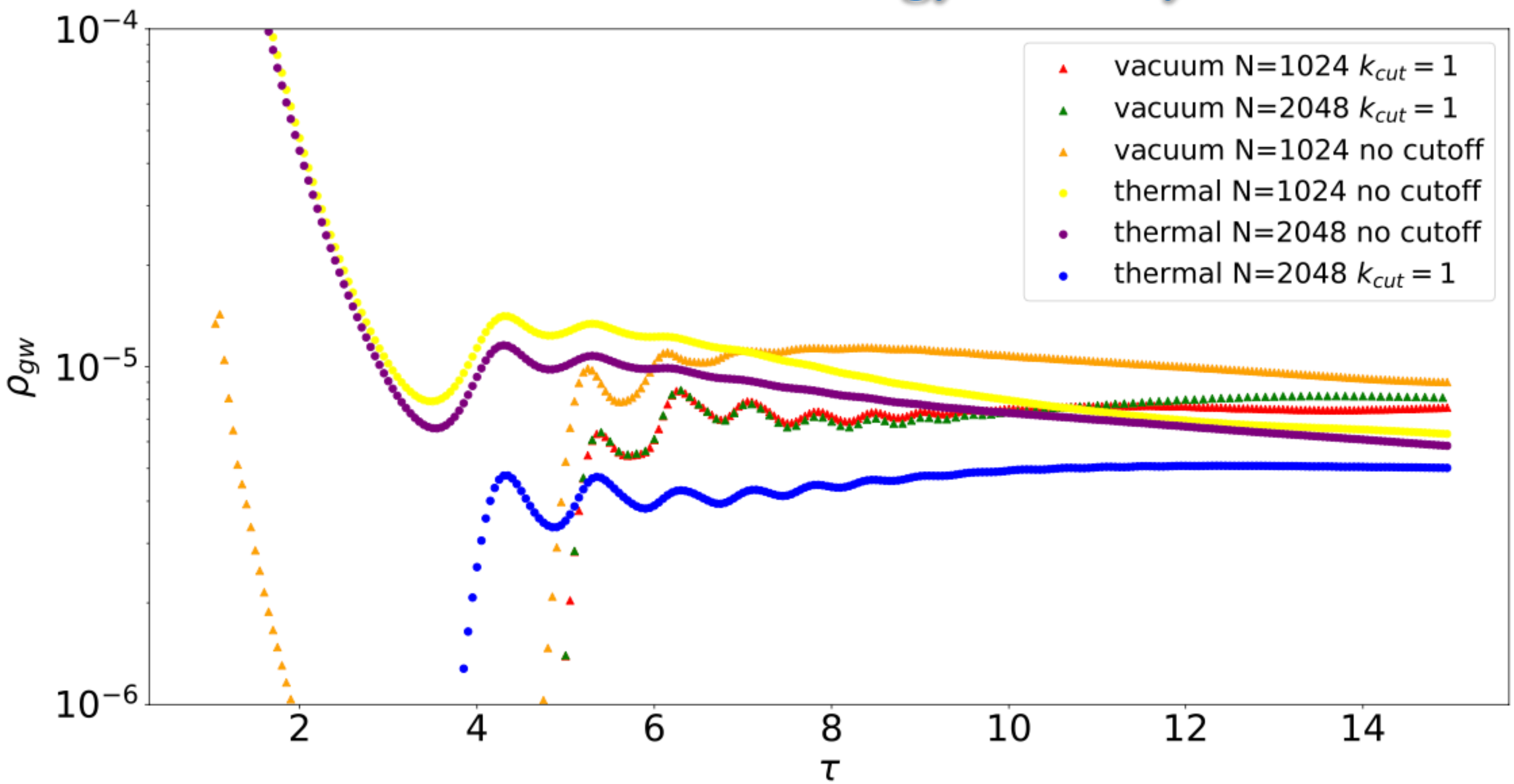

Figueroa, Florio, Torrenti, Valkenburg

CosmoLattice

Figure 6: The energy density of GWs in units of $\lambda\eta^4$ emitted by the domain wall network is obtained from numerical simulations on lattices with the grid numbers $N = 1024$ and $N = 2048$ starting from vacuum and thermal initial conditions with and without cutoffs. Conformal time τ is in units of $\frac{1}{\sqrt{\lambda}\eta}$. The expectation value η is set at $\eta = 6 \cdot 10^{16}$ GeV. Rescaling to arbitrary η is achieved by multiplying the energy density ρ_{gw} by $(\eta/6 \cdot 10^{16}\ \text{GeV})^2$.

Dankovsky, Babichev, Gorbunov, Ramazanov, Vikman (2024)

GW from constant tension DW

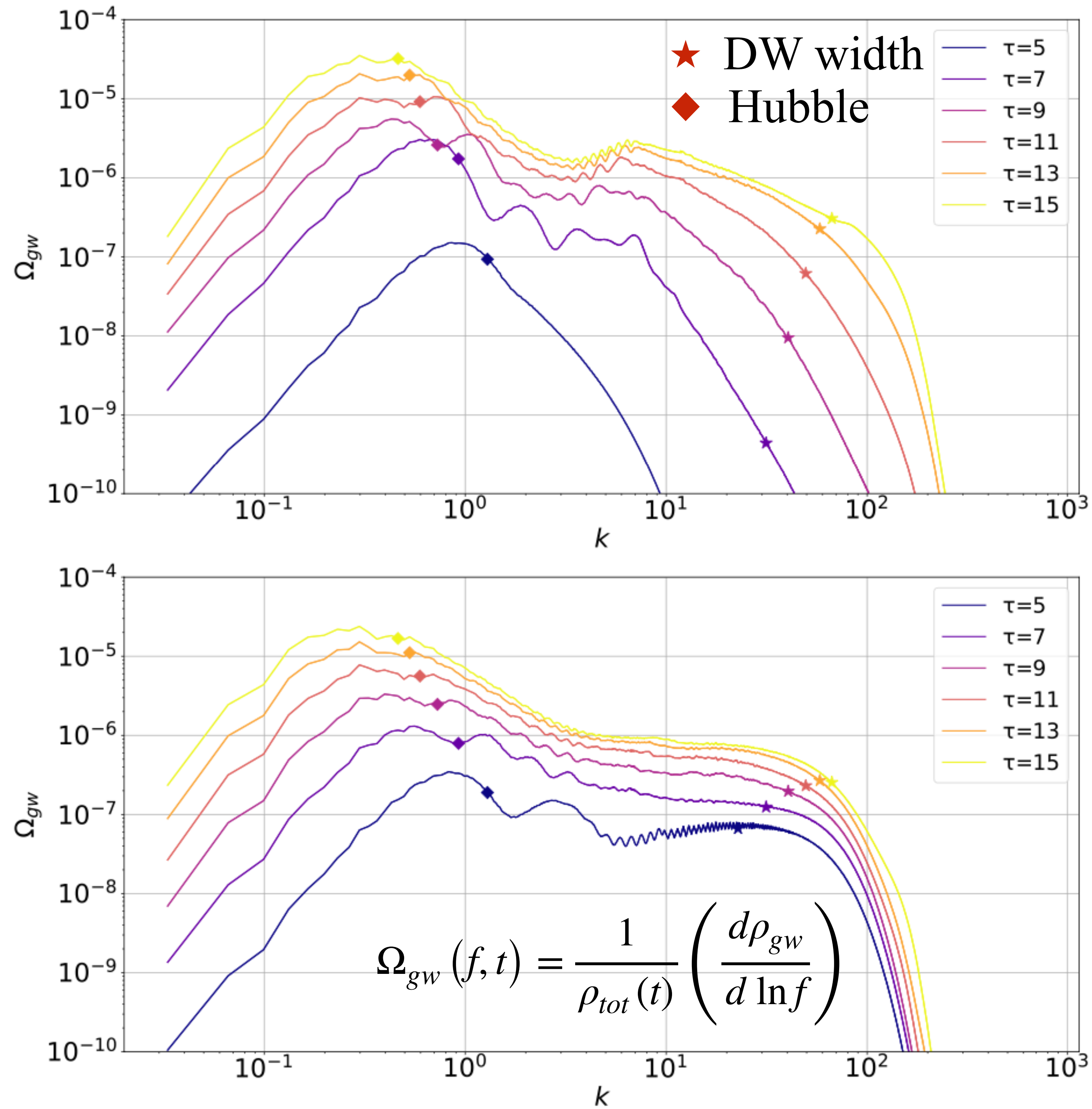

Figure 1: Spectrum of GWs emitted by the domain wall network at radiation domination starting with vacuum (top panel) and thermal (bottom panel) initial conditions defined in Eqs. (36) and (37), respectively. Conformal momenta and conformal times are in units of $\sqrt{\lambda}\eta$ and $\frac{1}{\sqrt{\lambda}\eta}$, respectively. The sharp upper cutoff at $k_{cut} = 1$ is applied in the case of vacuum initial conditions. The expectation value η is set at $\eta = 6 \cdot 10^{16}$ GeV. Rescaling to arbitrary η is achieved by multiplying the spectra by $(\eta/6 \cdot 10^{16}\ \text{GeV})^4$. Simulations have been performed on a lattice with a grid number $N = 2048$. The positions of diamonds correspond to the comoving Hubble scale $k = 2\pi Ha$ at the time associated with the corresponding curves, while stars show the inverse domain wall width $1/\delta_w$, i.e., $k = 2\pi a/\delta_w$.

Figueroa, Florio, Torrenti, Valkenburg

CosmoLattice

Dankovsky, Babichev, Gorbunov, Ramazanov, Vikman (2024)

cf.

Hiramatsu, Kawasaki, Saikawa (2013)

Yang Li, Ligong Bian, Yongtao Jia;
Yang Li, Ligong Bian, Rong-Gen Cai, Jing Shu (2023)

$$f_{peak} \simeq 0.7\, H_i \qquad f^0_{peak} \propto T_i$$

$$\Omega^{peak}_{gw} \sim \frac{\sigma^2_{dw}}{H^2_i} \propto \left(f^0_{peak}\right)^2$$

Melting Domain Walls

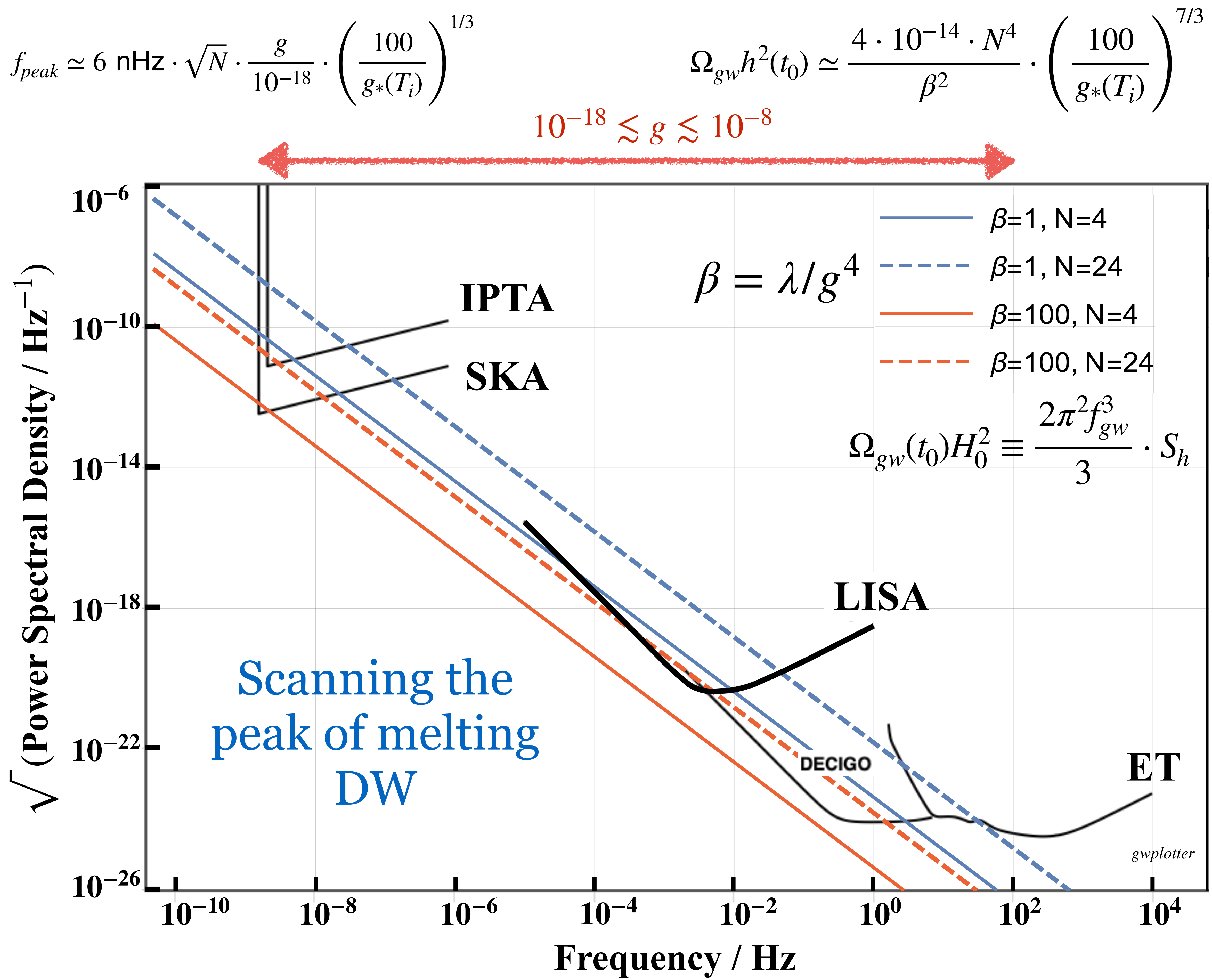

$f_{peak} \simeq 6\ \text{nHz} \cdot \sqrt{N} \cdot \frac{g}{10^{-18}} \cdot \left(\frac{100}{g_*(T_i)}\right)^{1/3}$
$\Omega_{gw}h^2(t_0) \simeq \frac{4 \cdot 10^{-14} \cdot N^4}{\beta^2} \cdot \left(\frac{100}{g_*(T_i)}\right)^{7/3}$
$10^{-18} \lesssim g \lesssim 10^{-8}$
$\beta = \lambda/g^4$
β=1, N=4
β=1, N=24
β=100, N=4
β=100, N=24
$\Omega_{gw}(t_0)H_0^2 \equiv \frac{2\pi^2 f_{gw}^3}{3} \cdot S_h$
IPTA
SKA
LISA
DECIGO
ET
Scanning the peak of melting DW
gwplotter
$\sqrt{(\text{Power Spectral Density / Hz}^{-1})}$
Frequency / Hz
10^{-6}
10^{-10}
10^{-14}
10^{-18}
10^{-22}
10^{-26}
10^{-10}
10^{-8}
10^{-6}
10^{-4}
10^{-2}
10^{0}
10^{2}
10^{4}

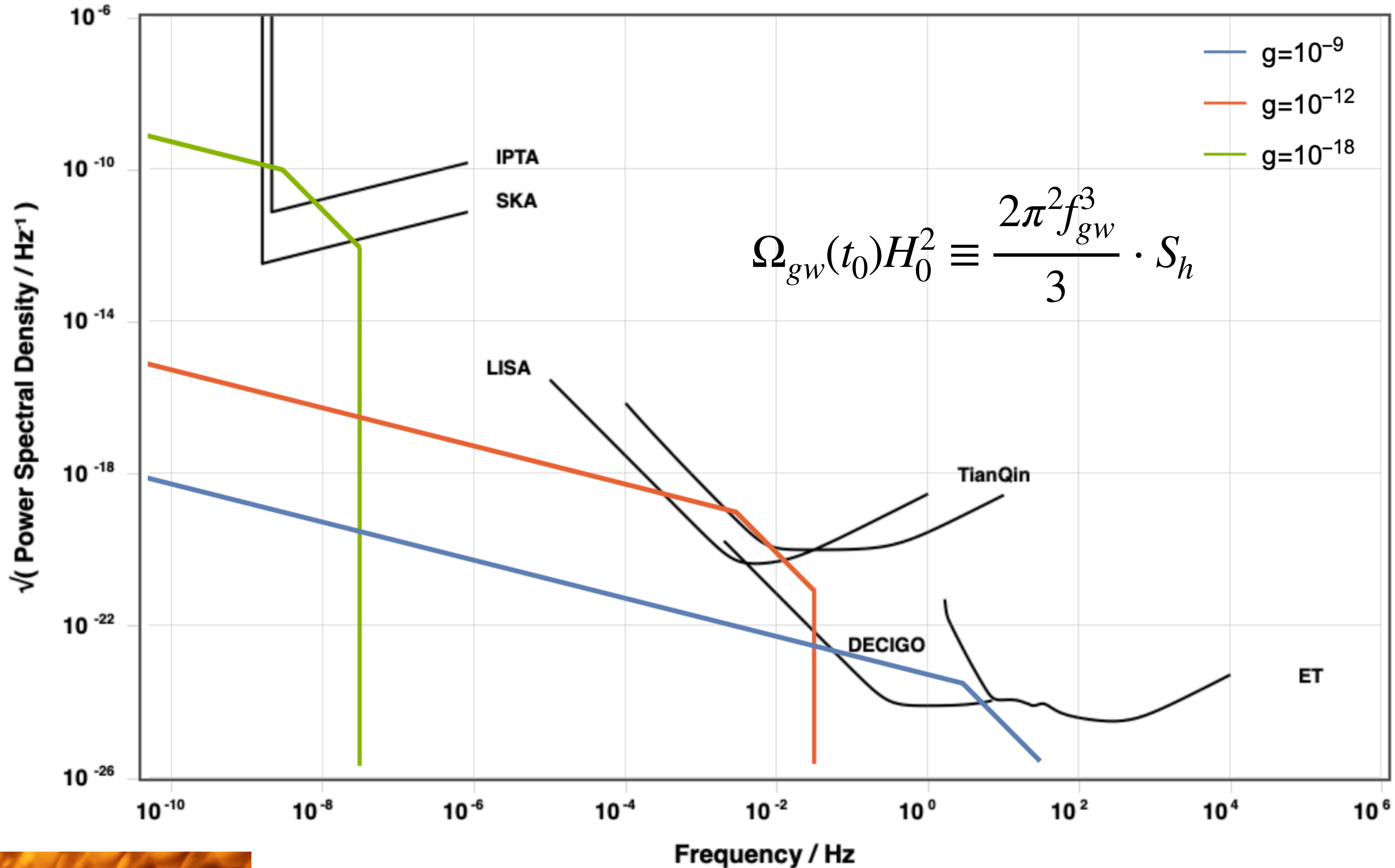

$$\Omega_{gw}(t_0)H_0^2 \equiv \frac{2\pi^2 f_{gw}^3}{3} \cdot S_h$$

$\Omega_{gw}(IR) \sim f^{2}$ $\Omega_{gw}(UV) \sim f^{-1}$ Cutoff $\ell = (\lambda/2)^{-1/2}\eta^{-1}$

Usual Domain Walls $\Omega_{gw}(IR) \sim f^{3}$

More on f^2 in IR

Dimensional analysis supported by simulation for constant tension

$$\Omega_{gw}\left(t_{now}\right)_{peak} \simeq A\left(\frac{f_{peak}}{F_{max}}\right)^2$$

energy is additive

Σ over t_{em} = Σ over f_{peak}

$$\delta\Omega_{gw}(f) = 2A\left(\frac{f_{peak}}{F_{max}^2}\right)\delta f_{peak}\left(\frac{f}{f_{peak}}\right)^p \frac{2}{1+\left(f/f_{peak}\right)^{p+q}}$$

for $f_{min} \ll f \ll F_{max}$

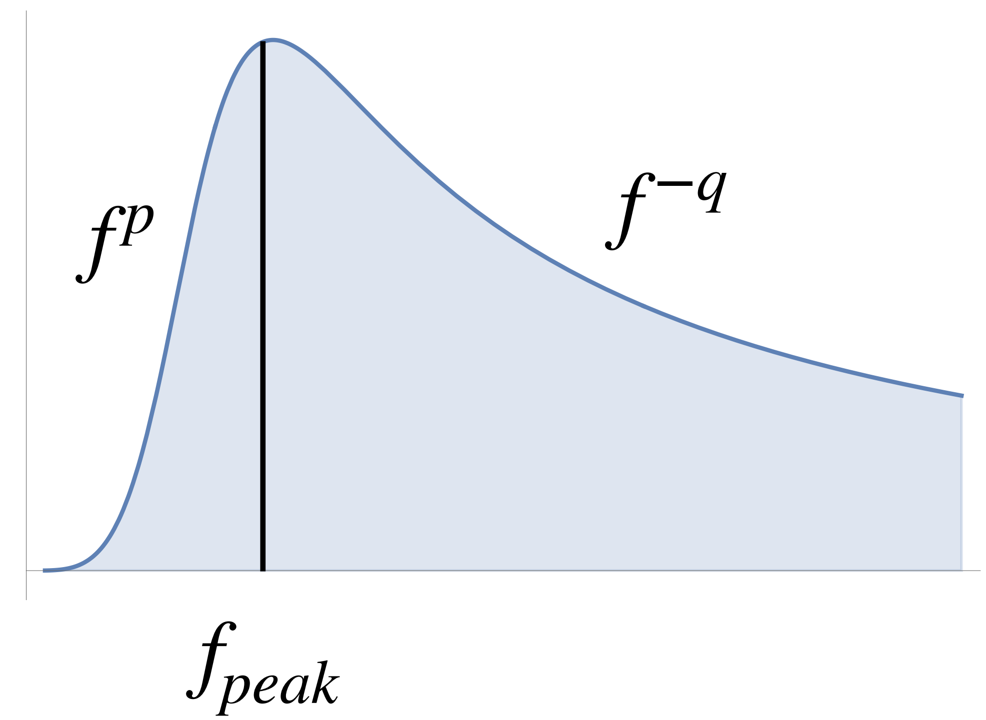

$$\Omega_{gw}(f) = \int_{f_{min}}^{F_{max}} \delta\Omega_{gw}(f) \propto \left(\frac{f}{F_{max}}\right)^2\left[1 - \mathcal{O}\left(\frac{f}{F_{max}}\right)^n - \mathcal{O}\left(\frac{f_{min}}{f}\right)^m\right]$$

e.g. J0437–4715 has a period of 0.005757451936712637 s with an error of 1.7×10^{-17} s

15 years of observations of 68 millisecond pulsars

The New York Times

The Cosmos Is Thrumming With Gravitational Waves, Astronomers Find

Radio telescopes around the world picked up a telltale hum reverberating across the cosmos, most likely from supermassive black holes merging in the early universe.

June 28, 2023

Share full article | 362

The Very Large Array on the Plains of San Agustin, N.M., one of three radio telescopes that worked with a global consortium to detect the timing of pulsars. NRAO/AUI/NSF

The Washington Post

In a major discovery, scientists say space-time churns like a choppy sea

The mind-bending finding suggests that everything around us is constantly being roiled by low-frequency gravitational waves

By Joel Achenbach and Victoria Jaggard

June 28, 2023 at 8:00 p.m. EDT

The Green Bank Observatory in Green Bank, W.Va., was among the observatories used to track pulsars as a way of detecting low-frequency gravitational waves. (Michael S. Williamson/The Washington Post)

Perfect for NANOGgrav

$$\Omega_{\rm GW}(f) = \Omega_{yr}\left(f/f_{\rm yr}\right)^{5-\gamma},$$

$$f_{yr} = 32\,\text{nHz}$$

$$\Omega_{yr} = \frac{2\pi^2}{3H_0^2}A^2 f_{yr}^2$$

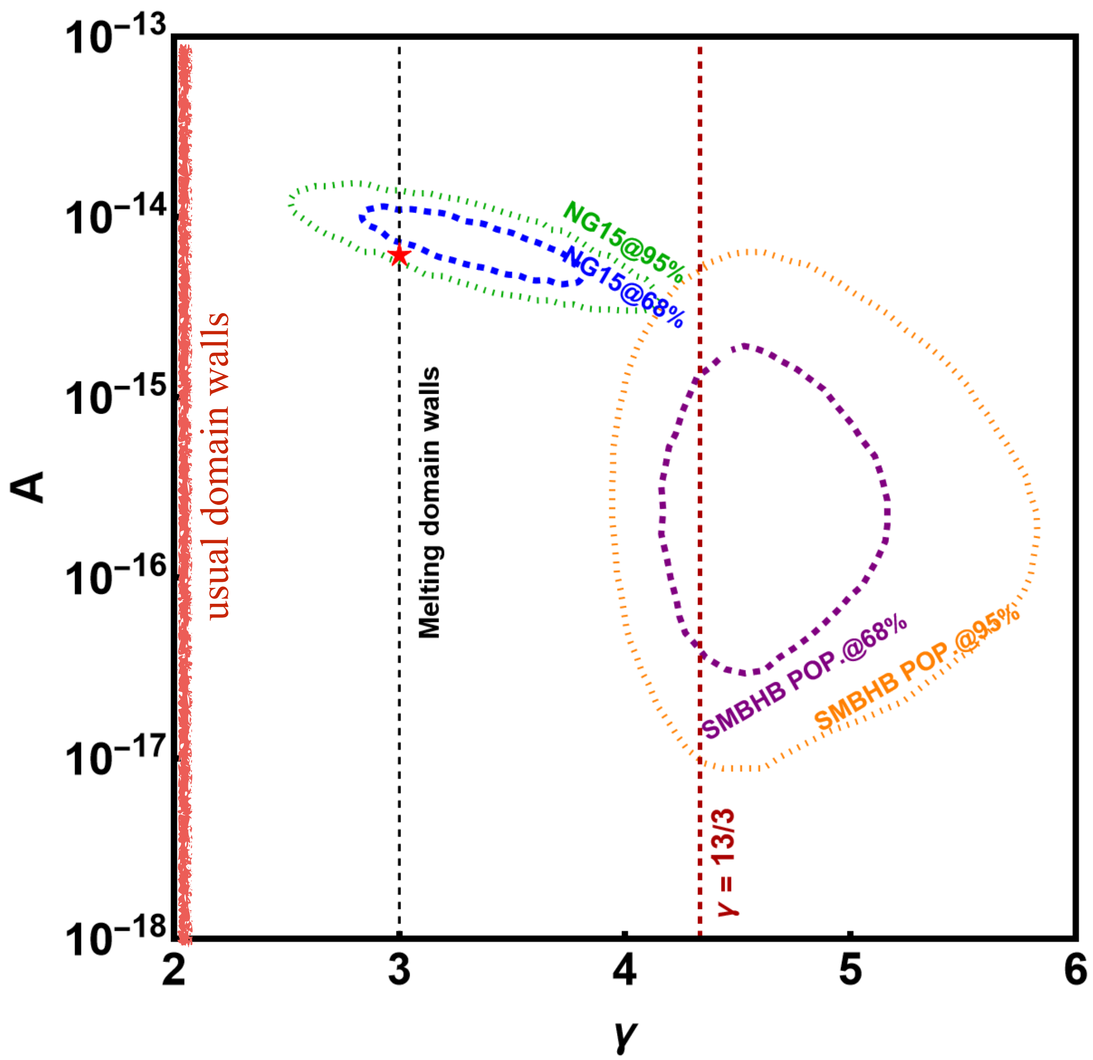

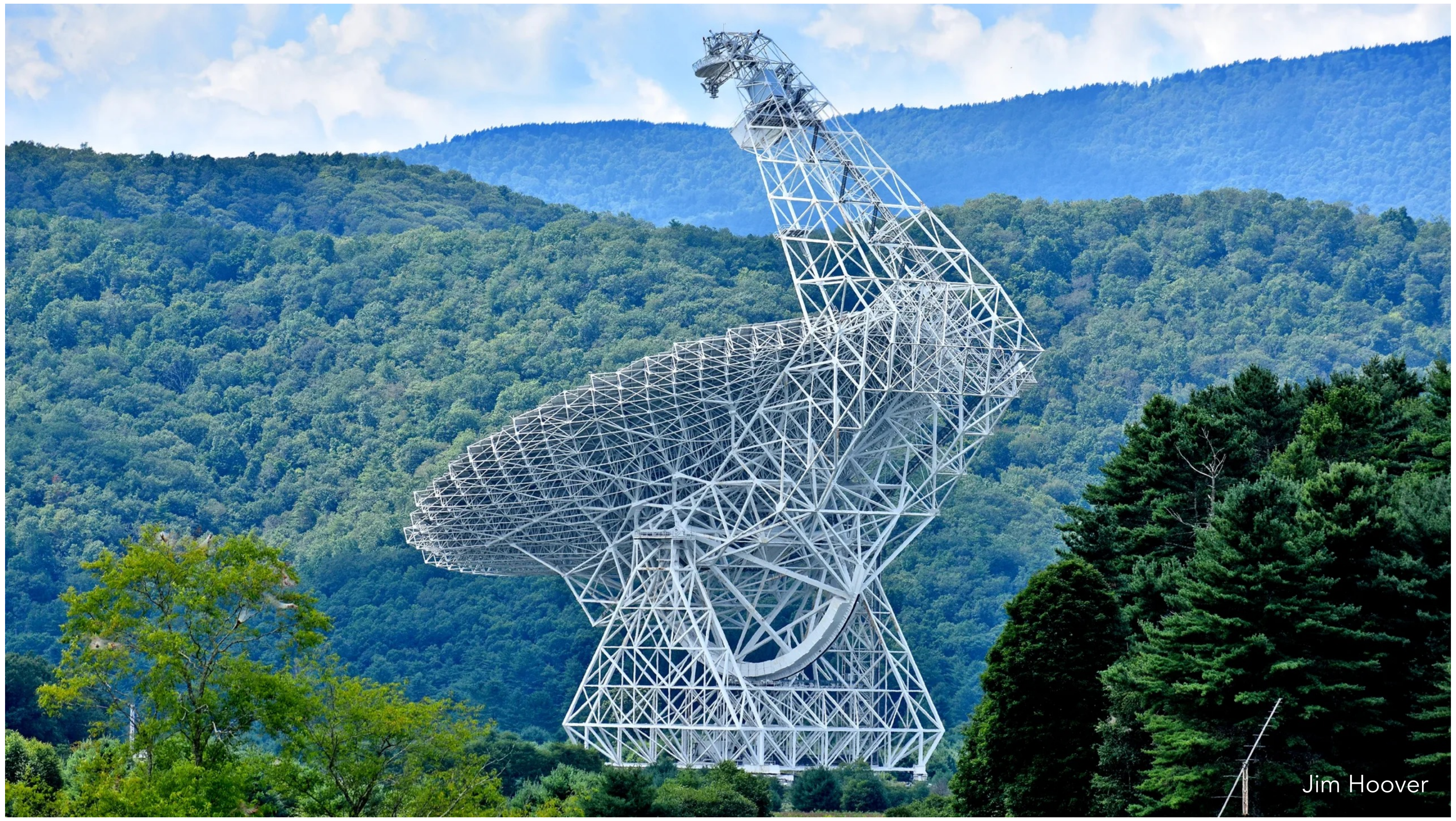

The 100-meter Green Bank Telescope, the world's largest fully steerable telescope and a core instrument for pulsar timing array experiment.

parameters $g = 10^{-18}$, $\beta = \lambda/g^4 = 1$, $N = 24$, $g_* = 75$

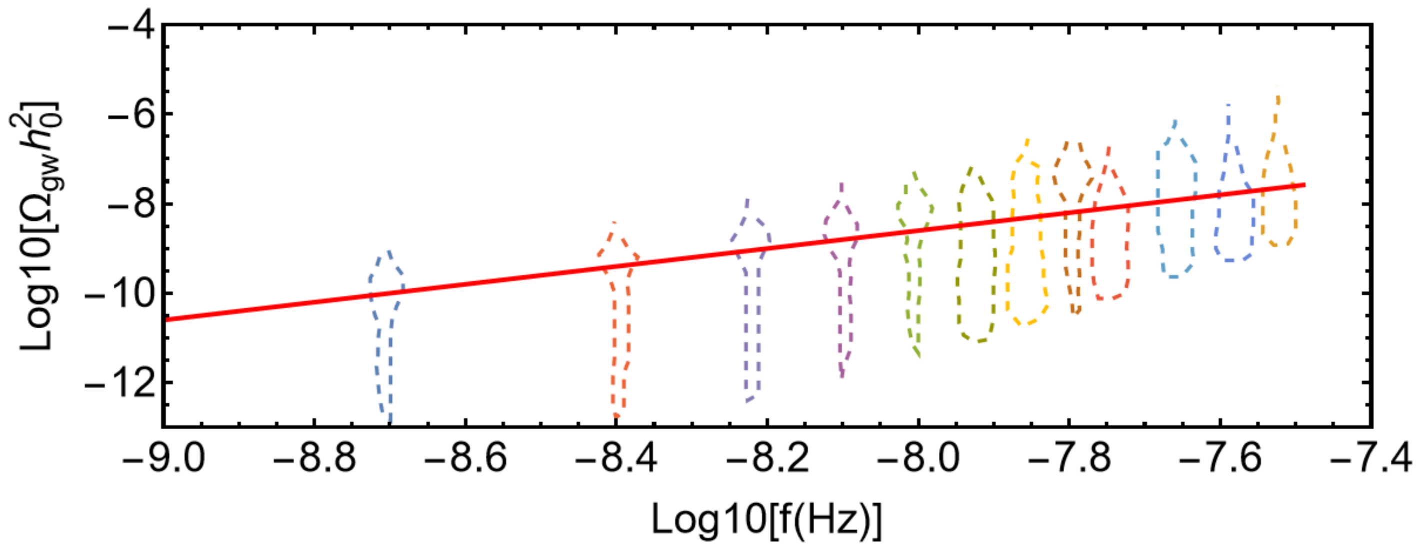

Inverse Phase Transition At Meltdown

$$\mathscr{L} = \frac{(\partial\chi)^2}{2} - \frac{\left(M^2 - \mu^2(t,\mathbf{x})\right)\cdot\chi^2}{2} - \frac{\lambda\chi^4}{4}$$

Early Universe

spontaneously Broken Phase with VEV slowly moving

Late Universe

DW melt down and disappear

then oscillations around restored symmetric vacuum

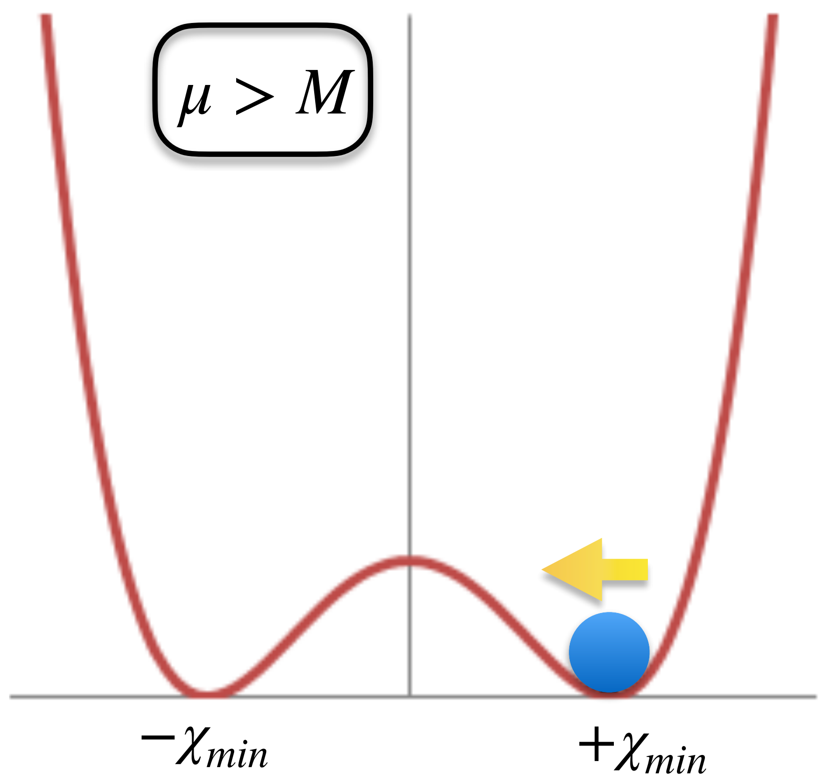

Tachyonic mass $\mu(t)$ slowly decreases / redshifts due to cosmological expansion

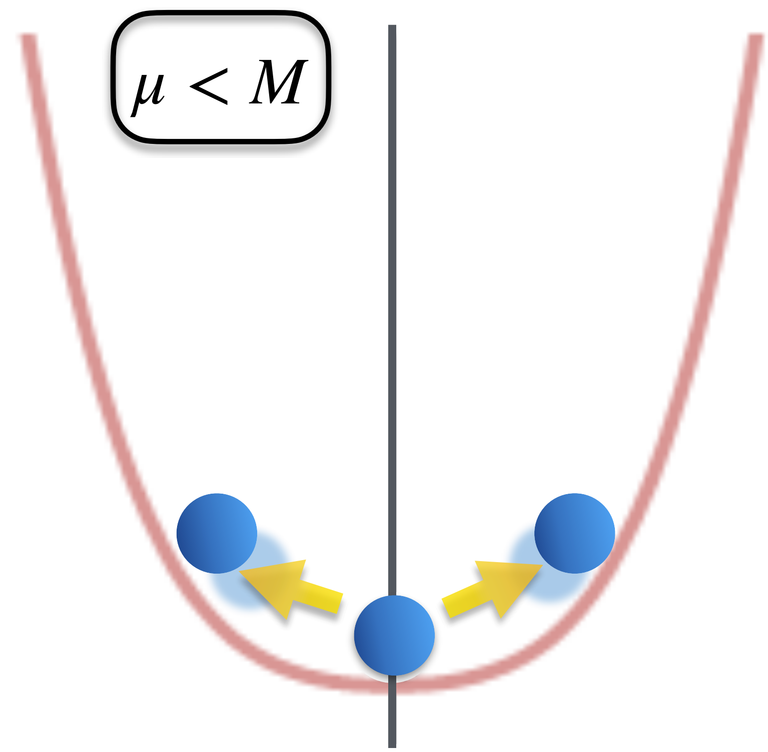

for Hubble parameter

$H < M$

scalar field traces vacuum $\quad \chi_{min}(t) = \sqrt{\dfrac{\mu^2(t) - M^2}{\lambda}}$ as long as $\left|\dfrac{\dot{M}_{eff}}{M_{eff}^2}\right| \ll 1$

Dynamics only depends on one single free dimensionless parameter

$$\ddot{\chi} + 3H\dot{\chi} + \left(M^2 - \frac{g^2 N T^2}{12}\right)\chi + \lambda\chi^3 = 0 \qquad \text{with} \qquad H = \frac{1}{2t} = \sqrt{\frac{\pi^2 g_*}{90}}\frac{T^2}{M_{pl}}$$

$$\frac{1}{\tau_\star^2}\left(\bar{\chi}'' + \frac{3}{2}\frac{\bar{\chi}'}{\tau}\right) + \left(1 - \frac{1}{\tau}\right)\bar{\chi} + \bar{\chi}^3 = 0$$

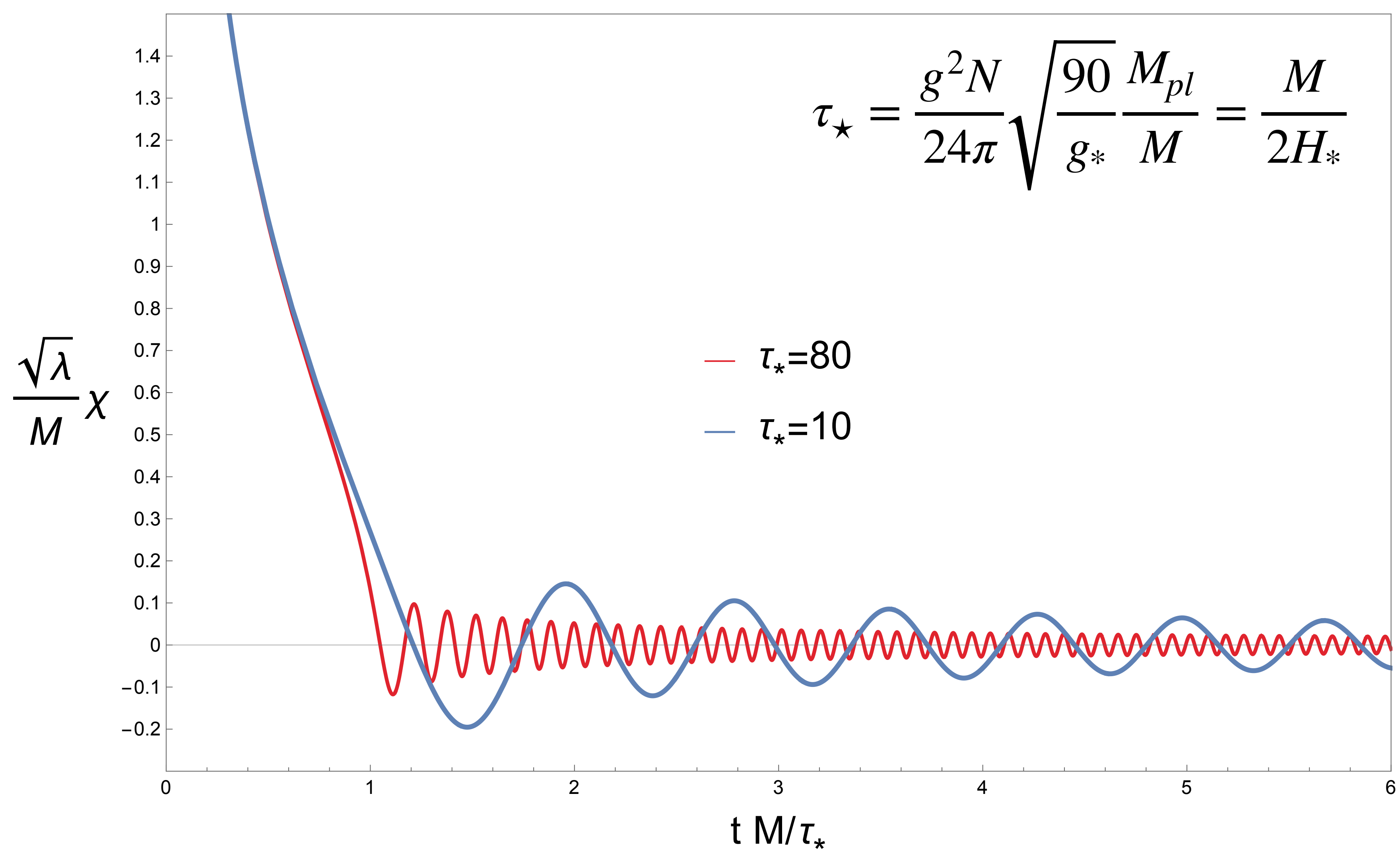

Allowed Parameter Space

$$M \simeq 10^{-13}\ \text{eV} \cdot \frac{\beta^{3/5}}{\sqrt{N}} \cdot \left(\frac{g_*(T_*)}{100}\right)^{2/5} \cdot \left(\frac{g}{10^{-18}}\right)^{7/5}$$

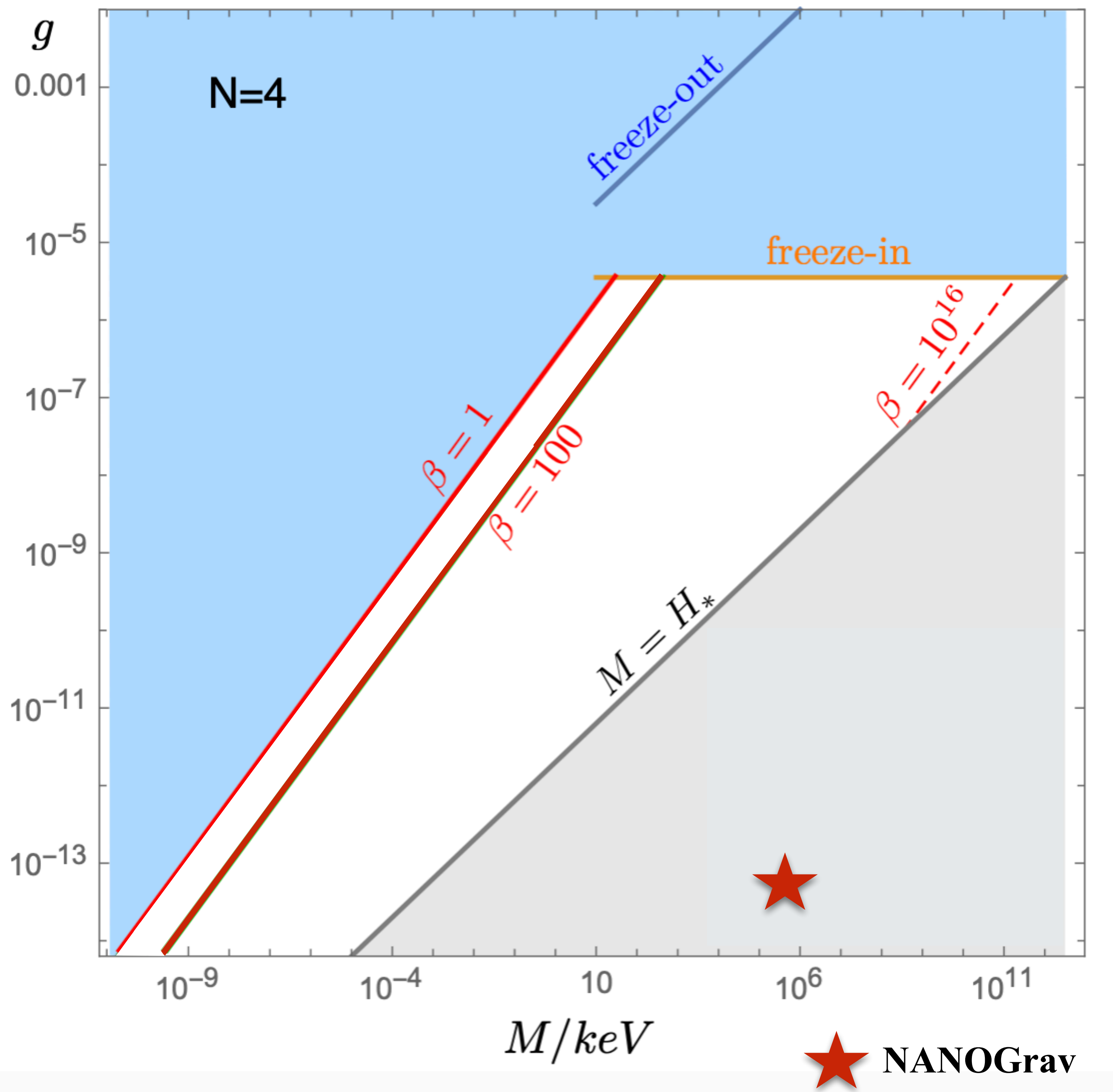

A bridge between NANOGrav and LIGO!

$$M_\chi \simeq 10^{-12}\ \mathrm{eV} \cdot B^{9/20} \cdot \left(\frac{g_*(T_{sym})}{100}\right)^{1/5} \cdot \left(\frac{g_*(T_i)}{100}\right)^{1/20} \cdot \left(\frac{m_\phi}{10\ \mathrm{MeV}}\right)^{1/2} \times \left(\frac{f_{peak}}{30\ \mathrm{nHz}}\right)^{6/5} \cdot \left(\frac{10^{-8}}{\Omega_{gw,peak}h_0^2}\right)^{3/20}$$

Superradiance for $M_{BH} \simeq 10^2 M_\odot$ → Just on on edge of LIGO!

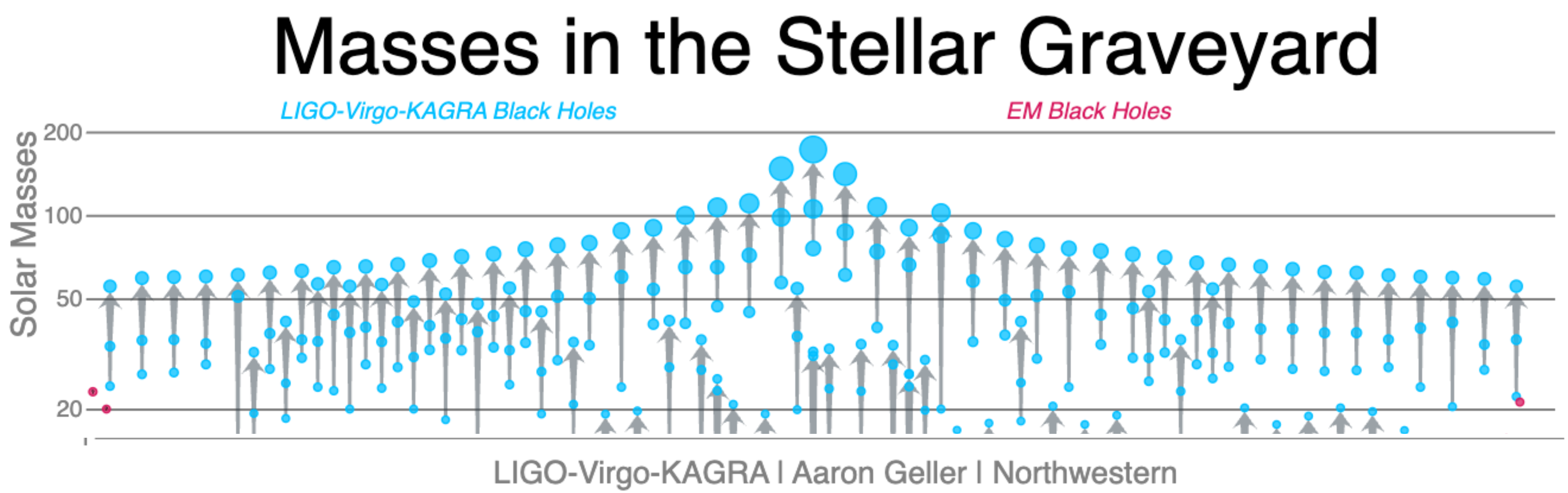


A highly promising path to the origins
of DM and NANOGrav signal
Thanks a lot for attention!